

Supporting Information

Two-dimensional Carbazole-based COFs for High-Performance Lithium-sulfur Batteries

Yuchen Xiao,^{abc} Shanyue Wei,^{abd} Xuan Wang,^{abd} Jia Liu,^{ab} Xiaowei Wu,^{ab*} Yiming Xie^{ad} and Can-Zhong Lu^{abc*}

^a State Key Laboratory of Structural Chemistry, Fujian Institute of Research on the Structure of Matter, Chinese Academy of Sciences, Fuzhou 350002, China.

^bXiamen Key Laboratory of Rare Earth Photoelectric Functional Materials, Xiamen Institute of Rare Earth Materials, Haixi Institutes, Chinese Academy of Sciences, Xiamen, 361021, China.

^cSchool of Physical Science and Technology, ShanghaiTech University, Shanghai, 201210, China.

^dEngineering Research Center of Environment-Friendly Function Materials, Ministry of Education, College of Materials Science & Engineering, Huaqiao University, Xiamen 361021, China.

Email: xmwuxiaowei@fjirsm.ac.cn; czlu@fjirsm.ac.cn

1. Materials and methods	1
2. Synthesis procedures	2
3. Preparation of cathode	4
4. Experimental data	5
5. Structure simulation data	10
6. Others	14
7. References	15

1. Materials and methods

All the chemicals are commercially available, and used without further purification.

Powder X-ray diffraction (PXRD): PXRD patterns were collected on a Rigaku Miniflex 600 using Cu K α radiation ($\lambda = 1.5418 \text{ \AA}$).

Fourier transform infrared (FT-IR): IR spectrum was measured on a Thermo Nicolet iS 50 FT-IR spectrometer with Universal ATR accessory between the ranges of 4000 to 500 cm^{-1} .

Solution nuclear magnetic resonance (NMR): Liquid state ^1H nuclear magnetic resonance spectroscopy was collected on a Bruker Avance III instrument with AS500 magnet equipped with a cryoprobe (500 MHz).

Scanning electron microscope (SEM): SEM images were collected using a JSM-IT500HR.

Solid-state nuclear magnetic resonance (ssNMR): Solid state ^{13}C cross polarization magic angle spinning nuclear magnetic resonance spectra (^{13}C CP-MAS NMR) were recorded on a JEOL JNM-ECA 400 MHz, 4.0 mm rotor, MAS of 10 kHz, recycle delay of 6.5 μs .

Transmission electron microscope (TEM): TEM images were obtained with a Hitachi H-7650.

The Brunauer-Emmett-Teller (BET): N_2 adsorption and desorption measurements were performed at 77 K using ASAP 2020, Micromeritics Instrument Corp, USA. Pore size distributions and pore volumes were derived from the adsorption isotherms.

UV-Vis diffuse reflectance spectroscopy (UV-Vis DRS): spectra were obtained by a UV-Vis spectrophotometer (UV-Vis-NIR Cary 5000) and the data were converted to Kubelka-Munk functions for the band gap extraction.

Thermogravimetric analysis (TGA): TGA was performed using a Mettler-Toledo TGA/DSC 1 under flowing Ar with 5 K min^{-1} ramp rate. Samples were heated in a Platinum pan (800 $^\circ\text{C}$, 10 $^\circ\text{C min}^{-1}$) under Ar flux (60 mL min^{-1}).

Elemental analysis (EA): EA data were collected using a Elementar Vario EL cube under CHN and CHNS model.

X-ray photoelectron spectroscopy (XPS): XPS was measured on a Thermo Scientific K-Alpha. Excitation source: Al K α ray ($h\nu = 1486.6\text{eV}$), Beam spot: 400 μm , the vacuum of the analysis room is better than 5.0E-7 mBar, operating voltage: 12 kV, filament current: 6 mA, full spectrum scanning: pass energy 150eV, step size 1eV; Narrow spectrum scanning: pass energy 50 eV, step size 0.1eV.

At least 5 cycles of signal accumulation for narrow spectrum. Binding energy correction: The energy standard of C1s=284.80 eV was used for charge correction.

Crystal structure modeling: Structural modeling of COFs was generated using the Materials Studio program (ver2019), the lattice model was geometrically optimized using force-field based method (Forcite, UFF, Ewald summations, Q_{eq}). Pawley fitting was conducted by using the Reflex module.

Density functional theory calculations: The adsorption energies of CBPA-PDA and CBPA-BZ complexed with and polysulfides (Li₂S_x, 2≤x≤8.) were calculated using DFT based on the Materials Studios (MS) software. The DMol3 module was used for calculating the energy between the COFs and LiPSs. Perdew Burke Ernzerh of functionals were used to calculate exchange and related energy components (GGA-PBE). The electronic energy was considered self-consistent when the energy change was smaller than 10⁻⁵ eV. A geometry optimization was considered convergent when the force change was smaller than 0.02 eV/Å. Considering the limitation of computing resources, the adsorption model is established by using CBPA coupled with four PDA/BZ monomers via imine linkage.

Electrochemical characterization: All electrochemical performances were measured at room temperature. The galvanostatic cycling performance tests were conducted on a Neware instrument at a voltage range of 1.7-2.8 V with different C rates. CHI 760E electrochemical workstation (Shanghai, China) was used to carry out the cyclic voltammetry (CV) measurements at a scan rate of 0.1 - 0.5 mV·s⁻¹, and the electrochemical impedance spectroscopy (EIS) tests with a voltage amplitude of 5 mV in the frequency range 0.1-10⁵ Hz. The specific capacity was calculated based on the weight of sulfur loaded in the cathode electrode.

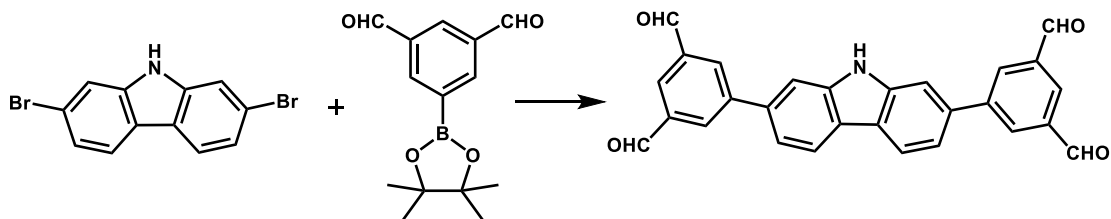
Calculation of the Diffusion Coefficient of Lithium Ions[1]: D_{Li+} could be calculated from the Randles–Sevcik equation, as shown below

$$I_p = 2.69 \times 10^5 n^{\frac{3}{2}} A D^{\frac{1}{2}} C v^{\frac{1}{2}}$$

where I_p represents the current of each peak (A), n is the number of electrons transferred during the reaction (for LSBs, $n = 2$), A is the surface area of the cathode (cm²), D is the lithium-ion diffusion coefficient (cm² s⁻¹), C is the concentration of Li in the electrolyte (mol L⁻¹), and v represents the scanning rate (V s⁻¹).

2. Synthesis procedures

5,5'-(9H-carbazole-2,7-diyl)diisophthalaldehyde (CBPA)



650 (2 mmol, 1 eq.) mg 2,7-dibromo-9H-carbazole, 1300 mg (5 mmol, 2.5 eq.) 1,3-Benzenedicarboxaldehyde,5-(4,4,5,5-tetramethyl-1,3,2-dioxaborolan-2-yl) (was synthesized according to the literature[2]), 2211 mg (16mmol, 8eq.) K_2CO_3 and 23 mg $Pd(PPh_3)_4$ were weighed and packed in 120 mL pressure bottle and adding 30 mL 1,4-dioxane and 6 mL H_2O as solvent. The reaction mixture was vacuumed and filled with inert gas three times and stirred at 120 °C for 48 h. After cooling to room temperature, the mixture was filtrated followed by rinsing with water and alcohol, and drying in vacuum to give a yellow powder of 5,5'-(9H-carbazole-2,7-diyl) diisophthalaldehyde (CBPA) (yield: 88.3%). 1H NMR (DMSO- d_6 , 500 MHz, ppm): δ -11.59 (s, 1H), 10.24 (s, 4H), 8.63 (d, 4H), 8.39 (d, 2H), 8.35 (d, 2H), 7.96 (d, 2H), 7.68 (dd, 2H). ^{13}C NMR (125 MHz, DMSO, ppm) δ 193.28, 143.17, 141.55, 137.91, 136.08, 133.70, 128.09, 122.77, 121.83, 118.64, 109.92.

CBPA-PDA

PDA (10.8 mg, 0.1 mmol) and CBPA (21.5 mg, 0.05 mmol) were added into a 10 mL Pyrex tube; then, a mixture of *o*-dichlorobenzene (*o*-DCB, 1.0 mL), *n*-butanol (*n*-BuOH, 1.0 mL), and acetic acid (aq 6 M, 0.2 mL) was added into this Pyrex tube. The Pyrex tube was sealed after being evacuated under vacuum for three pump–thaw cycles in a liquid nitrogen bath. After that, the sealed Pyrex tube was placed in a vacuum oven at 120 °C for 3 days. The solid was isolated by centrifugation, washed with ethyl acetate, and further purified by Soxhlet extraction with tetrahydrofuran, methanol, and trichloromethane. The sample was then transferred to a vacuum chamber and evacuated to 20 mTorr at 50 °C for 24 h, yielding COFs as dark green powders (yield: 28.1 mg, 87.0%).

CBPA-BZ

BZ (18.4 mg, 0.1 mmol) and CBPA (21.5 mg, 0.05 mmol) were added into a 10 mL Pyrex tube; then, a mixture of *o*-dichlorobenzene (*o*-DCB, 1.0 mL), *n*-butanol (*n*-BuOH, 1.0 mL), and acetic acid (aq 6 M, 0.2 mL) was added into this Pyrex tube. The Pyrex tube was sealed after being evacuated under vacuum for three pump–thaw cycles in a liquid nitrogen bath. After that, the sealed Pyrex tube was placed in a vacuum oven at 120 °C for 3 days. The solid was isolated by centrifugation, washed with ethyl acetate, and further purified by Soxhlet extraction with tetrahydrofuran, methanol, and trichloromethane. The sample was then transferred to a vacuum chamber and evacuated to 20 mTorr at 50 °C for 24 h, yielding COFs as chartreuse powders (yield: 33.1 mg, 83.6%).

3. Preparation of cathode

Lithium polysulfides (LiPS) adsorption:

The sublimated sulfur and Li_2S were dissolved in dimethyl ether solution with a molar ratio of 5:1, and stirred at 60°C until the liquid turned yellow (0.4 mol/L) to obtain Li_2S_6 solution. Then $0.1 \text{ mL } 0.4 \text{ mol L}^{-1}$ poly-lithium sulfide solution was mixed with 9.9 mL dimethyl ether solution to obtain 10 mL diluted Li_2S_6 /DME test solution. For the next 20 min , 20 mg of COF was put into 10 mL of Li_2S_6 /DME solutions next to vigorous stirring, then leave to rest. All of the experiments were carried out in an argon-filled glove box. Finally, 0.2 mL of supernatant was taken and diluted with 2.0 mL DME to measure the UV-visible absorbance.

S@COFs:

COF and sulfur powder were added with a weight ratio of 4:6 to a mortar, grinding for 30 minutes to blend thoroughly. The mixture was then sealed in a glass tube filled with nitrogen and heated to 155°C at the heating rate of 2°C min^{-1} for 12 hours , to obtain S@COFs.

Li-S Cell Assembly and Electrochemical Measurements:

The S@COF, Ketjen black and polyvinylidene fluoride (PVDF) binder at a mass ratio of 7:2:1 combined with N-methyl-2-pyrrolidone (NMP) as a dispersant to make the cathode slurry, then the slurry was uniformly cast on the aluminum foil and dried at 60°C for 12 h , and the acquired piece was sliced into a film disk of 12 mm in diameter. The areal mass loading of sulfur was approximately 0.45 mg/cm^2 . The CR2025 coin cells were assembled with Li metal as an anode, and 1 mol/L LITFSI + 1 wt\% lithium nitrate (LiNO_3) dissolved in the mixed solvent of dimethoxyethane (DME) and 1,2-dioxolane (DOL) (1:1, v:v) as an electrolyte, and a microporous polypropylene film (Celgard 2400) was employed as a separator. About $15 \text{ }\mu\text{L}$ of electrolyte was added for each coin cell. In addition, the coin cells were gathered in a glove box with low oxygen and water content filled with argon. The galvanostatic cycling performance tests were conducted at 25°C on Neware battery test equipment in the voltage range of $1.7\text{--}2.8 \text{ V}$ with different C rates.

4. Experimental data

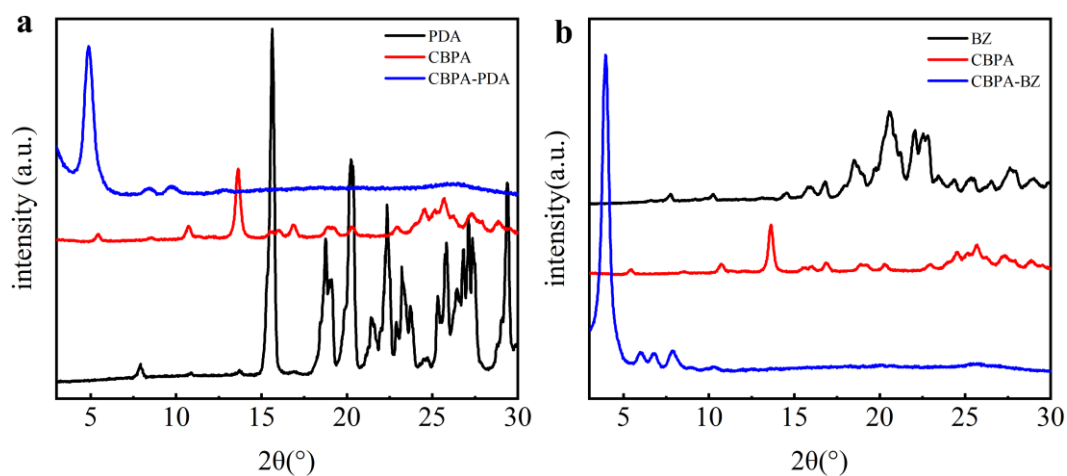


Figure S1. PXRD of (a) CBPA-PDA and (b) CBPA-BZ

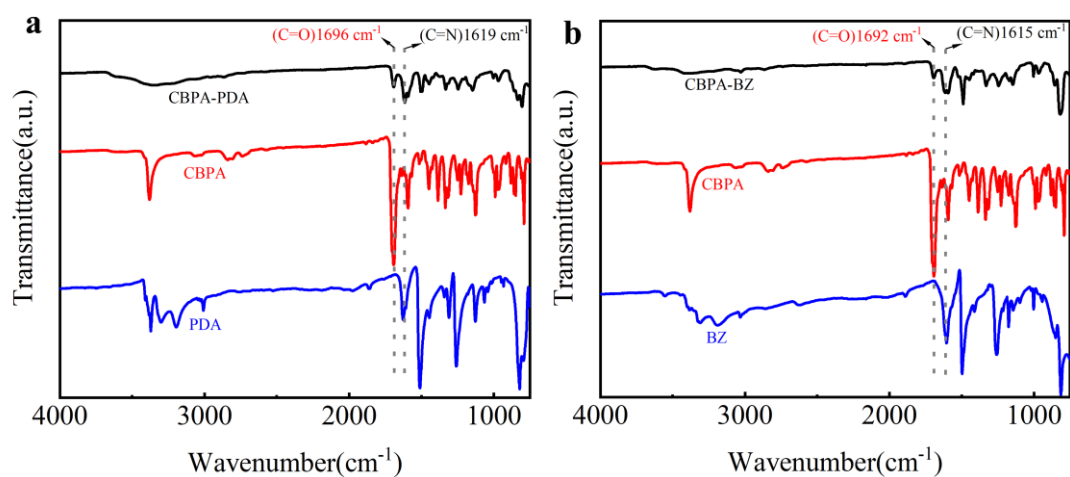


Figure S2. FT-IR curve of (a) CBPA-PDA and (b) CBPA-BZ

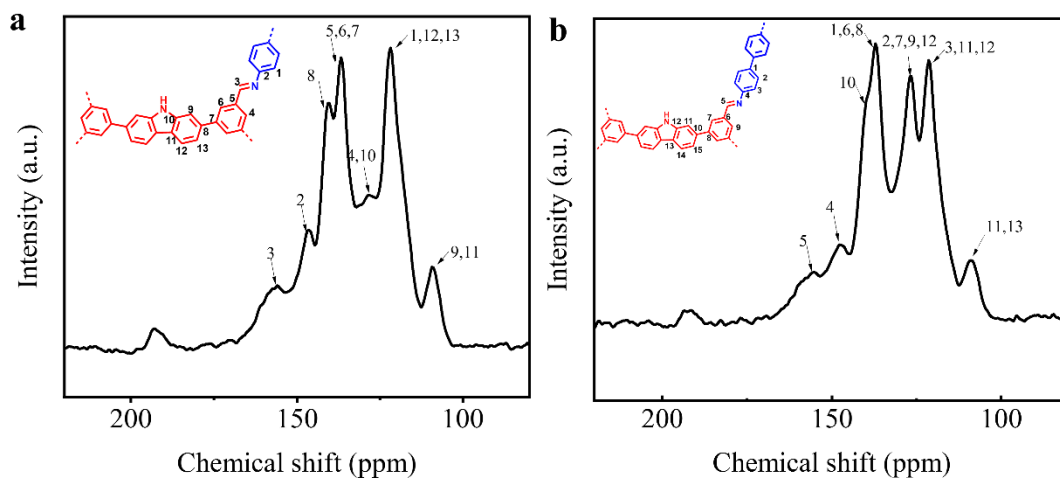


Figure S3. Solid-state ^{13}C NMR spectra of (a) CBPA-PDA and (b) CBPA-BZ

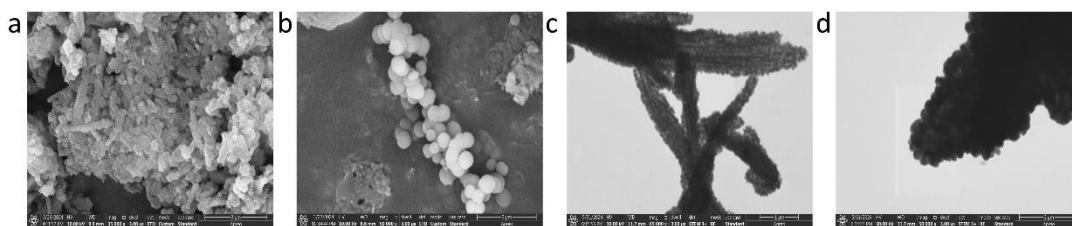


Figure S4. SEM of (a) CBPA-PDA and (b) CBPA-BZ, TEM of (b) CBPA-PDA and (d) CBPA-BZ

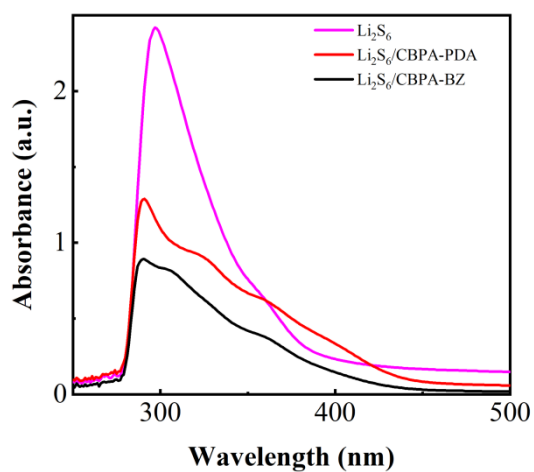


Figure S5. UV-vis spectra of Li_2S_6 solution after the adsorption by CBPA-PDA and CBPA-BZ

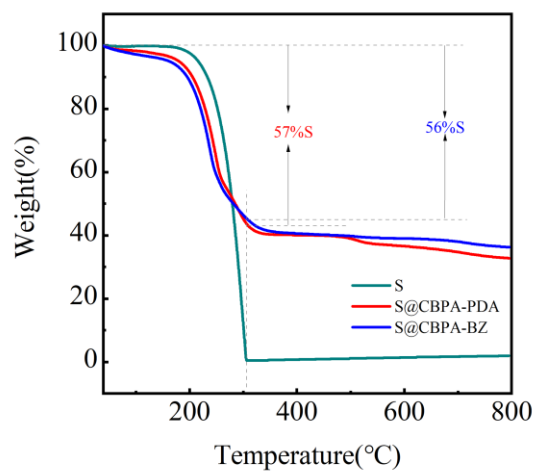


Figure S6. The TGA curves of S, S@CBPA-PDA and S@CBPA-BZ

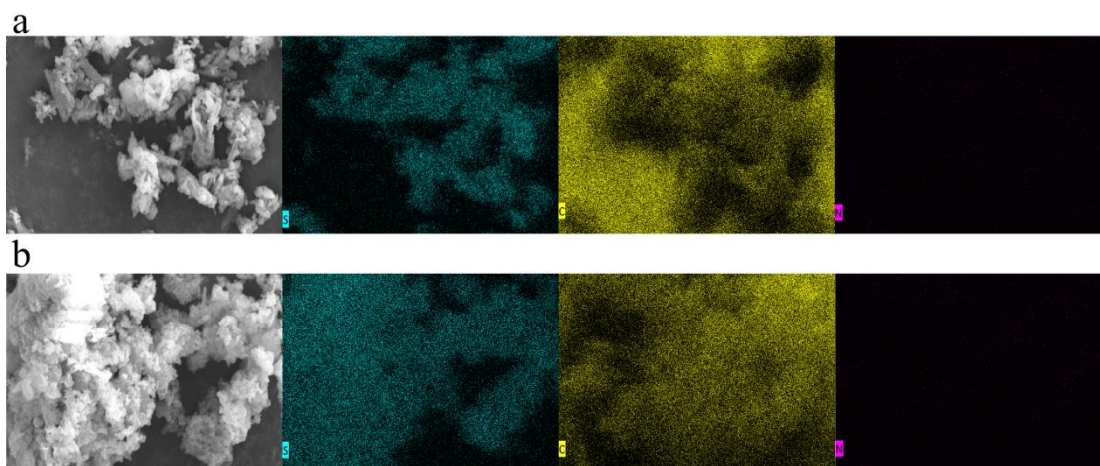


Figure S7. SEM and EDX elemental mapping image of (a) S@CBPA-PDA and (b) S@CBPA-BZ

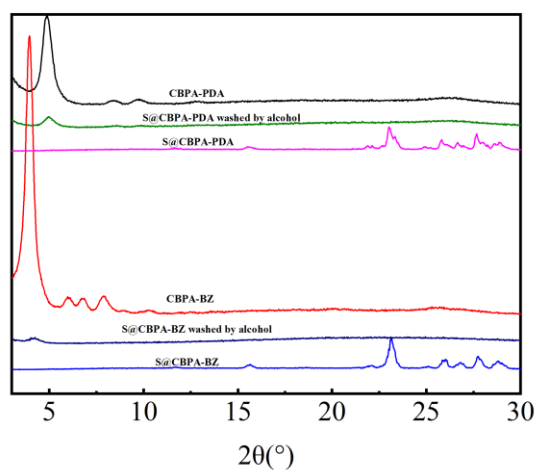


Figure S8. PXRD of S@COFs, S@COFs (washed by alcohol) and COFs

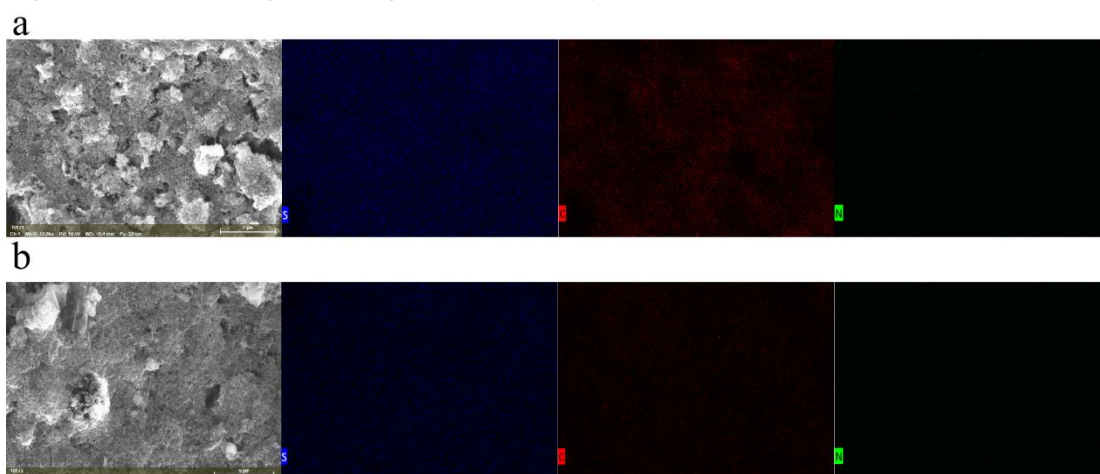


Figure S9. SEM and EDX elemental mapping image of (a) S@CBPA-PDA and (b) S@CBPA-BZ electrodes

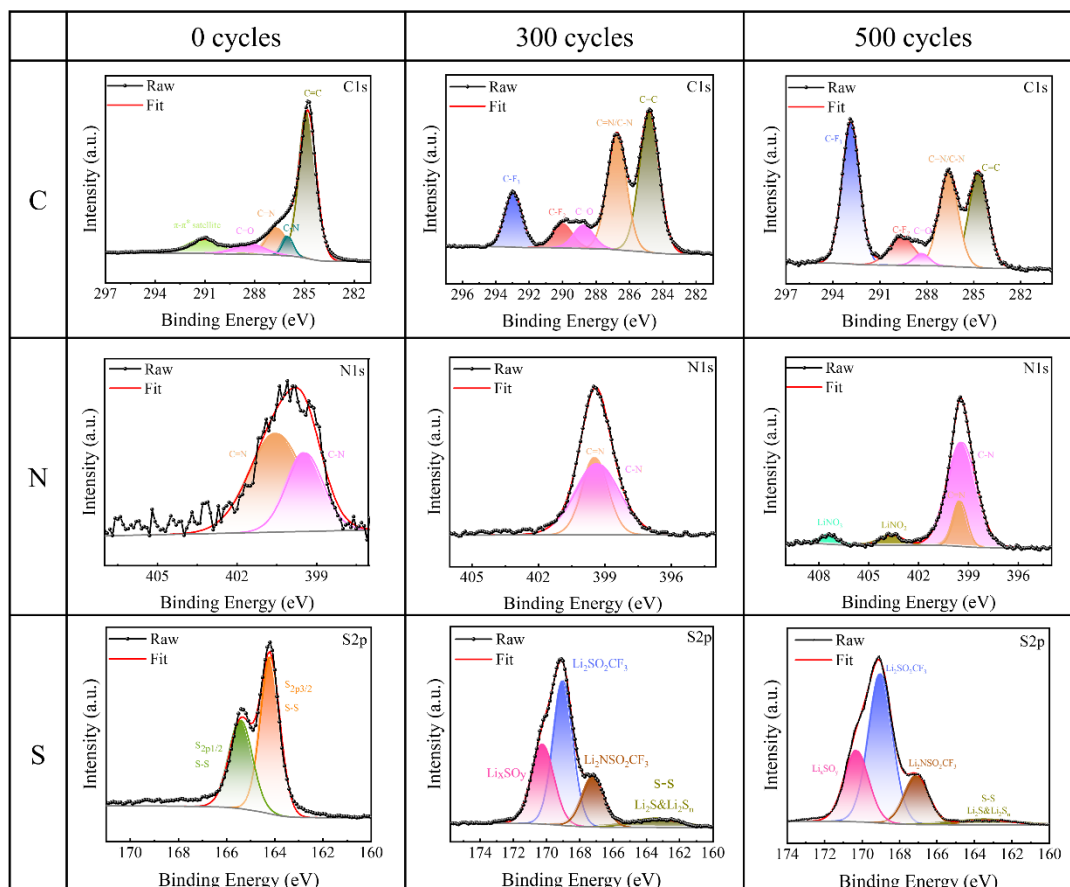


Figure S10. X-ray photo-electron spectra of S@CPBA-PDA electrode about C1s, N1s and S2p

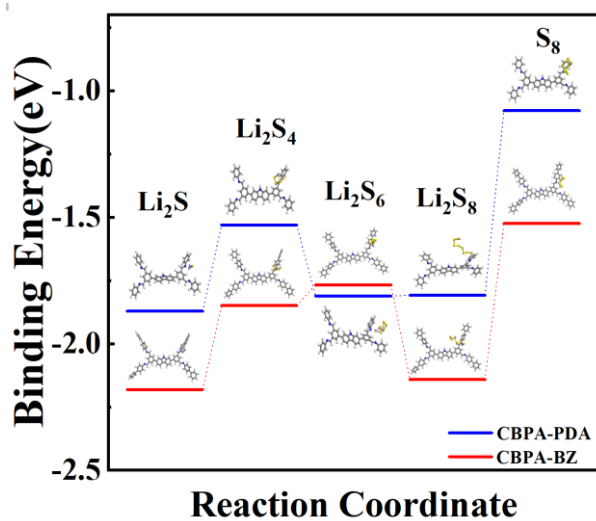


Figure S11. Binding energy between LiPSs and representative models from CBPA coupled with four PDA/BZ monomers via imine linkages.

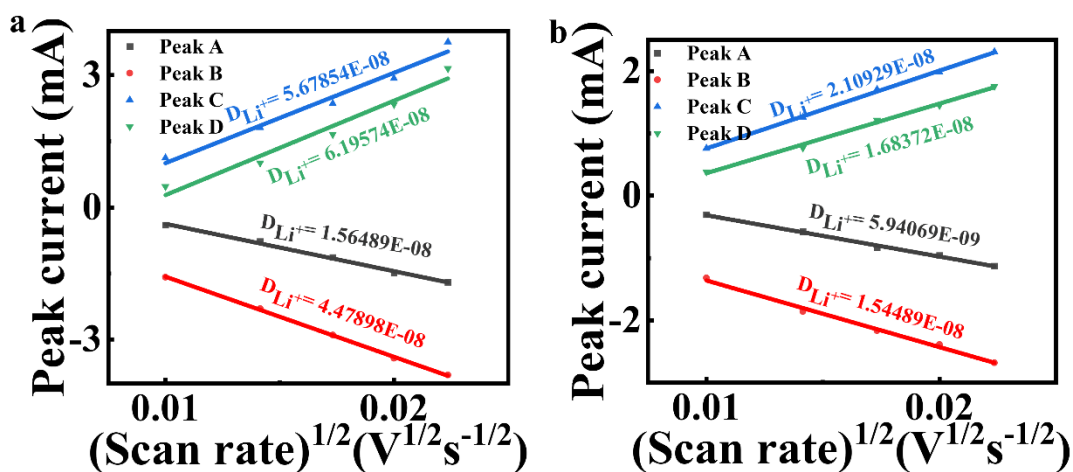


Figure S12. Linear relationship with the square root of the scanning rate and peak current of (a) S@CBPA-PDA and (b) S@CBPA-BZ electrode.

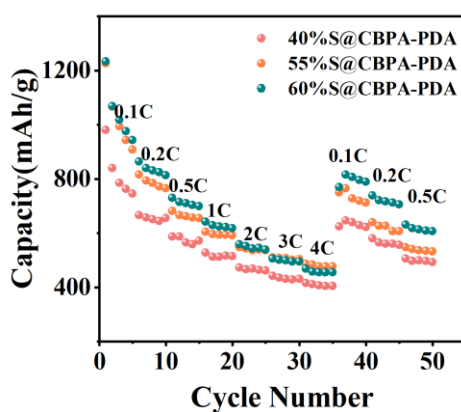


Figure S13. Rate capacity of S@CBPA-PDA cathodes with different sulfur-loaded samples

Table S1. Elemental analyses (C, H and N) for COFs

Sample	Calculated/Found %			Calculated C/N	Found C/N
	C	H	N		
CBPA-PDA	83.47/82.63	4.35/5.87	12.18/11.5	6.86	7.18
CBPA-BZ	85.83/84.92	4.54/5.36	9.63/9.72	8.91	8.74

Table S2. Elemental analyses (C, H, N and S) for S@COFs

Sample	Found %			
	C	H	N	S
S@CBPA-PDA	30.69	2.64	4.42	62.25
S@CBPA-BZ	32.96	2.55	3.67	60.82

5. Structure simulation data

Table S3. Fractional atomic coordinates for simulated CBPA-PDA

Space group: P21				
a = 3.66 Å, b = 36.81 Å, c = 21.61 Å				
$\alpha = \gamma = 90.0^\circ$, $\beta = 104.0^\circ$				
Atom label	Atom type	x	y	z
C1	C	0.51316	0.70636	0.37215
N2	N	0.40493	0.69296	0.42026
C3	C	0.35521	0.71673	0.4706
C4	C	0.51707	0.72987	0.58372
C5	C	0.46689	0.70481	0.53374
N6	N	-0.01246	0.20561	-0.12484
C7	C	-0.1296	0.22969	-0.08091
C8	C	-0.23426	0.23904	0.02447
C9	C	-0.14982	0.21603	-0.0215
C10	C	0.00962	0.31393	0.28087
C11	C	0.12887	0.35024	0.27855
C12	C	0.59189	0.68545	0.31878
C13	C	0.53773	0.64781	0.30882
C14	C	0.50081	0.56559	0.2835
C15	C	0.42686	0.52944	0.26397
C16	C	0.21288	0.43317	0.26747
C17	C	0.30094	0.46937	0.25691
C18	C	-0.214	0.29773	0.22635
C19	C	0.0217	0.3701	0.22066
C20	C	0.14451	0.40857	0.21492
C21	C	0.30886	0.48115	0.19673
C22	C	0.9147	0.71587	0.1761
C23	C	-0.43503	0.29405	0.11078
N24	N	-0.31784	0.30161	0.06038
C25	C	-0.30516	0.27616	0.01101
C26	C	-0.22022	0.26656	-0.0952
C27	C	-0.3002	0.28954	-0.04906
N28	N	0.57894	0.79433	0.61944
C29	C	0.45812	0.7673	0.57072
C30	C	0.24599	0.75344	0.45857
C31	C	0.29754	0.77843	0.50842
C32	C	0.79114	0.69099	0.22012
C33	C	0.7411	0.65371	0.20973

C34	C	-0.30108	0.31588	0.16853
C35	C	-0.19501	0.35214	0.16594
C36	C	0.18192	0.42152	0.15451
C37	C	0.25686	0.45796	0.14495
C38	C	0.43478	0.58129	0.17099
C39	C	0.37679	0.54489	0.15334
C40	C	0.71452	0.70629	0.27403
C41	C	0.60384	0.63149	0.25282
C42	C	0.514	0.59232	0.2363
C43	C	0.38136	0.51969	0.20099
C44	C	0.12363	0.28994	0.3365
N45	N	0.623	-0.00072	0.69967
H46	H	0.56689	0.73516	0.37114
H47	H	0.61856	0.72022	0.63223
H48	H	0.54263	0.67665	0.54391
H49	H	-0.22333	0.22815	0.07139
H50	H	-0.08532	0.18777	-0.01012
H51	H	0.3096	0.36234	0.32075
H52	H	0.42674	0.63218	0.34245
H53	H	0.54989	0.57231	0.33358
H54	H	0.18778	0.4249	0.31429
H55	H	-0.29511	0.26947	0.22765
H56	H	0.90746	0.74439	0.18685
H57	H	-0.56024	0.26787	0.11538
H58	H	-0.22863	0.27825	-0.1413
H59	H	-0.35042	0.3181	-0.05948
H60	H	0.14177	0.76338	0.41036
H61	H	0.2369	0.80687	0.49817
H62	H	0.81654	0.64238	0.16842
H63	H	-0.28121	0.36577	0.1204
H64	H	0.15542	0.40358	0.11409
H65	H	0.27731	0.46763	0.09859
H66	H	0.4104	0.60071	0.13273
H67	H	0.32105	0.5368	0.10371
H68	H	0.75275	0.73531	0.2813
H69	H	-0.04191	0.26552	0.33588
H70	H	0.62993	-0.0011	0.65163

Table S4. Fractional atomic coordinates for simulated CBPA-BZ

Space group: P21
a = 4.00 Å, b = 45.00 Å, c = 25.60 Å

$\alpha = \gamma = 90.0^\circ, \beta = 93.3^\circ$				
Atom label	Atom type	x	y	z
C1	C	0.32586	0.66805	0.37066
N2	N	0.53172	0.67694	0.40839
C3	C	0.45386	0.69823	0.44749
C4	C	0.60241	0.71975	0.53247
C5	C	0.61989	0.69637	0.49686
C6	C	-0.37936	0.27797	-0.02944
C7	C	-0.52305	0.2967	0.05542
C8	C	-0.52204	0.27371	0.01877
C9	C	-0.00219	0.35761	0.25897
C10	C	0.11282	0.38715	0.25671
C11	C	0.45917	0.65644	0.32256
C12	C	0.41527	0.62685	0.30646
C13	C	0.44536	0.56183	0.27681
C14	C	0.39824	0.53301	0.25744
C15	C	0.18145	0.45489	0.25327
C16	C	0.28058	0.4844	0.24687
C17	C	-0.21008	0.34641	0.21785
C18	C	0.02742	0.40497	0.21233
C19	C	0.14929	0.43626	0.2085
C20	C	0.33954	0.49557	0.19813
C21	C	0.91316	0.6901	0.21283
C22	C	-0.45753	0.34807	0.12845
N23	N	-0.31064	0.34632	0.08465
C24	C	-0.38087	0.32453	0.04446
C25	C	-0.25247	0.30615	-0.04134
C26	C	-0.25156	0.3291	-0.0045
C27	C	0.42339	0.74582	0.5188
C28	C	0.26451	0.72376	0.43424
C29	C	0.25012	0.7474	0.46958
C30	C	0.75068	0.6674	0.24433
C31	C	0.72074	0.63749	0.22914
C32	C	-0.28653	0.36319	0.17317
C33	C	-0.16821	0.39232	0.17025
C34	C	0.22496	0.44813	0.15902
C35	C	0.31695	0.47798	0.15355
C36	C	0.49573	0.57853	0.18665
C37	C	0.45638	0.54926	0.16845
C38	C	0.61765	0.67654	0.29079
C39	C	0.54666	0.61683	0.25937

C40	C	0.49733	0.58535	0.24102
C41	C	0.41103	0.52701	0.20487
C42	C	0.10554	0.33625	0.30031
N43	N	0.6819	0.00693	0.71378
H44	H	0.07145	0.6755	0.36877
H45	H	0.74596	0.71815	0.56953
H46	H	0.7757	0.67728	0.50676
H47	H	-0.61789	0.2919	0.09313
H48	H	-0.62326	0.25227	0.02876
H49	H	0.27801	0.3957	0.28817
H50	H	0.27274	0.61216	0.33013
H51	H	0.44307	0.56549	0.31847
H52	H	0.12213	0.44701	0.29156
H53	H	-0.29763	0.32363	0.21909
H54	H	0.92406	0.71248	0.22822
H55	H	-0.66208	0.33337	0.1365
H56	H	-0.13422	0.30989	-0.07777
H57	H	-0.1333	0.35006	-0.01294
H58	H	0.14144	0.72602	0.3957
H59	H	0.10752	0.76704	0.45823
H60	H	0.83739	0.63053	0.19411
H61	H	-0.23407	0.40505	0.13533
H62	H	0.2136	0.43432	0.12439
H63	H	0.36821	0.48703	0.11569
H64	H	0.51679	0.59582	0.15774
H65	H	0.45343	0.5443	0.12708
H66	H	0.63891	0.69961	0.30281
H67	H	0.72967	0.00529	0.67424
C68	C	2.5613	1.27174	1.44524
C69	C	2.50812	1.30068	1.46405
C70	C	2.44488	1.32431	1.42909
C71	C	2.4285	1.31922	1.3751
C72	C	2.50335	1.29069	1.35648
C73	C	2.57035	1.26729	1.39113
N74	N	2.31526	1.34236	1.33949
C75	C	0.33115	0.75253	2.06501
C76	C	0.20576	0.72535	2.04507
C77	C	0.11632	0.7027	2.07897
C78	C	0.14841	0.70681	2.13313
C79	C	0.29568	0.73323	2.15311
C80	C	0.38419	0.75591	2.11931

N81	N	0.0123	0.68461	2.16636
H82	H	2.4981	1.30476	1.5056
H83	H	2.38965	1.34618	1.44393
H84	H	2.50163	1.2864	1.31489
H85	H	2.61984	1.24546	1.37556
H86	H	0.161	0.72215	2.00335
H87	H	0.34017	0.73661	2.1947
H88	H	0.48923	0.77631	2.13556
H89	H	0.00589	0.68242	2.0631
H90	H	0.00817	0.31387	0.29612

6. Others

Table S5. A summary of covalent organic frameworks as sulfur-loading materials for LSBs

Materials	Sulfur loading (wt.%)	Capacity (CD ^a /RC ^b)	Voltage range (vs. Li/Li ⁺)	Cycling performance (CD/CN ^c /RC)	Ref
S@CBPA-PDA	60	0.1/1232 4.0/468	1.7–2.8	1.0/500/461	This work
S@CBPA-BZ	60	0.1/987 4.0/436	1.7–2.8	1.0/500/429	
S/Co/Zr-NC@TpPa	60	0.2/1120 3.0/701	1.7–2.8	1.0/500/502	[3]
COF-MF@S-60%	60	0.1/1266 2.0/743	1.7–2.8	0.5/300/749	[4]
S-Co@COF-Ph-OH	/	0.1/1350 2.0/678	/	0.5/200/655	[5]
COF-SH@PVDF-HFP	60	0.1/1359 2.0/688.7	1.7–2.8	2.0/800/569	[6]
DAAQ-COF@S	70	0.1/1182 4.0/616.8	1.7-2.8	2.0/500/525	[7]
S/Co-NC@TpBD-Me	75	0.2/1178 5.0/543	1.7-2.8	1.0/500/636	[8]
R-COF-BTD@S	60	0.1/1594 2.0/731	1.7-2.6	0.5/200/872	[9]
COF-Tr-BA@S	60	0.1/1400 2.0/714	/	0.5/200/627	[10]
S@EB-COF-PS	70	0.1/1136 5.0/661	/	0.5/500/555	[11]
S-COF-V	67	0.2/1400 6.0/431	1.7-2.8	1.0/1000/416	[12]

COF-301@S	60	0.2/940 1.0/603	1.7-2.8	0.5/500/411	[13]
SO ₃ ⁻ COF@Al ₂ O ₃ /S	90	0.05/1141	1.7-2.8	1.0/500/466	[14]
COF-PA-AI/S	40	0.1/920 2.0/518	1.7-2.8	0.5/200/665	[15]
3DOM TpPa-1 @Co/TiO _x Ny/S	80	0.2/1173 5.0/638	1.7-2.8	1.0/500/817	[16]
S@TFPB-TAA	58	0.1/1288 2.0/537	1.7-2.8	0.5/400/482	[17]
S@TFPB-TAB	61	0.1/1192 2.0/586	1.7-2.8	0.5/400/480	
COF-SQ-Ph-S	40	0.1/1370 2.0/733	1.7-2.8	0.5/150/618	[18]
S@THZ-DMTD	82	0.1/1149 2.0/499	1.7-2.8	0.5/200/556	[19]
S-DUT-177	62	0.06/720 0.6/276	1.2-2.8	0.3/500/76.6 ^d	[20]
COF-F-S	75	0.1/1120 2.0/325	1.7-2.8	1.0/1000/257	[21]
S@3D-flu-COF	70	0.2/1249 5.0/764	1.7-2.8	0.5/100/1024	[22]
S@3D-scu-COF-1	70	0.2/1025 5.0/713	1.7-2.8	2.0/500/71%	[23]
S@3D-scu-COF-2	70	0.2/1025 5.0/757	1.7-2.8	2.0/500/83%	[23]

^a CD: current density (C), ^b RC: reversible capacity (mA h g⁻¹), ^c CN: cycle number, ^d retention rate

7. References

1. Y. Zhu, J. Yang, X. Qiu, M. Li, G. He, Q. Wang, Z. Xie, X. Li, H. Yu. *ACS applied materials & interfaces*, 2021, **13**, 60373.
2. D. Wetzell, U. Lüning. *European Journal of Organic Chemistry*, 2022, **2022**, e202200983.
3. T. Lin, H. Wang, X. Du, D. Zhang, Z. Zhang, G. Liu. *Electrochimica Acta*, 2022, **412**, 140156.
4. X. Hu, J. Jian, Z. Fang, L. Zhong, Z. Yuan, M. Yang, S. Ren, Q. Zhang, X. Chen, D. Yu. *Energy Storage Materials*, 2019, **22**, 40.
5. Z. Wu, L. Feng, J. Luo, Y. Zhao, X. Yu, Y. Li, W. Wang, Z. Sui, X. Tian, Q. Chen. *Journal of Colloid and Interface Science*, 2023, **650**, 1466.
6. L. Bi, J. Xiao, Y. Song, T. Sun, M. Luo, Y. Wang, P. Dong, Y. Zhang, Y. Yao, J. Liao, S. Wang, S. Chou. *Carbon Energy*, 2024.
7. S. Cai, R. Ma, W. Ke, H. Zhang, Y. Liu, M. Jiao, Y. Tian, Y. Fang, M. Wu, Z. Zhou. *Chemical*

- Engineering Journal*, 2024, **491**, 151979.
8. B. Du, Y. Luo, Y. Yang, W. Xue, G. Liu, J. Li. *Chemical Engineering Journal*, 2022, **442**, 135823.
9. Y. Ge, Y. Meng, L. Liu, J. Li, X. Huang, D. Xiao. *Green Energy & Environment*, 2023.
10. Y. Liang, T. Xia, Z. Chang, W. Xie, Y. Li, C. Li, R. Fan, W. Wang, Z. Sui, Q. Chen. *Chemical Engineering Journal*, 2022, **437**, 135314.
11. X. F. Liu, H. Chen, R. Wang, S. Q. Zang, T. C. Mak. *Small*, 2020, **16**, 2002932.
12. Q. Jiang, Y. Li, X. Zhao, P. Xiong, X. Yu, Y. Xu, L. Chen. *Journal of Materials Chemistry A*, 2018, **6**, 17977.
13. Z. Li, H.-Y. Zhou, F.-L. Zhao, T.-X. Wang, X. Ding, B.-H. Han, W. Feng. *Chinese Journal of Polymer Science*, 2020, **38**, 550.
14. B. Jia, W. Liu, C. Yao, W. Xie, Y. Xu. *Chemical Communications*, 2024, **60**, 6435.
15. X. Liu, M. Xia, Y. Zhao, T. Xia, Y. Li, J. Xiao, Z. Sui, Q. Chen. *Materials Today Chemistry*, 2022, **23**, 100664.
16. H. Wang, J. Jiang, T. Wan, Y. Luo, G. Liu, J. Li. *Journal of Colloid and Interface Science*, 2023, **638**, 542.
17. Z. Wang, X. Wu, S. Wei, Y. Xie, C.-Z. Lu. *Chemistry of Materials*, 2024, **36**, 2412.
18. Y. Liang, M. Xia, Y. Zhao, D. Wang, Y. Li, Z. Sui, J. Xiao, Q. Chen. *Journal of Colloid and Interface Science*, 2022, **608**, 652.
19. R. Yan, B. Mishra, M. Traxler, J. Roeser, N. Chaoui, B. Kumbhakar, J. Schmidt, S. Li, A. Thomas, P. Pachfule. *Angewandte Chemie International Edition*, 2023, **62**, e202302276.
20. S. Haldar, M. Wang, P. Bhauriyal, A. Hazra, A. H. Khan, V. Bon, M. A. Isaacs, A. De, L. Shupletsov, T. Boenke. *Journal of the American Chemical Society*, 2022, **144**, 9101.
21. D.-G. Wang, N. Li, Y. Hu, S. Wan, M. Song, G. Yu, Y. Jin, W. Wei, K. Han, G.-C. Kuang. *ACS applied materials & interfaces*, 2018, **10**, 42233.
22. W. Liu, K. Wang, X. Zhan, Z. Liu, X. Yang, Y. Jin, B. Yu, L. Gong, H. Wang, D. Qi. *Journal of the American Chemical Society*, 2023, **145**, 8141-8149.
23. W. Liu, L. Gong, Z. Liu, Y. Jin, H. Pan, X. Yang, B. Yu, N. Li, D. Qi, K. Wang. *Journal of the American Chemical Society*, 2022, **144**, 17209-17218.